The Effects of Cell Culture Conditions on Premature Hydrolysis of Traceless Ester-Linked Disulfide Linkers

D. J. Blevins, R. Nazir, S. M. H. Dabri, M. Akbari, and J. E. Wulff

2022

The effects of cell culture conditions on premature hydrolysis of traceless ester-linked disulfide linkers

Derek J. Blevins[a], Rashid Nazir[a], Seyed Mohammad Hossein Dabiri[b], Mohsen Akbari[b], Jeremy E. Wulff[a,c,*]

[a] Department of Chemistry, University of Victoria, Victoria, BC V8W 3V6, Canada

[b] Laboratory for Innovations in MicroEngineering (LiME), Department of Mechanical Engineering, University of Victoria, Victoria, BC V8P 5C2, Canada

[c] Centre for Advanced Materials and Related Technology (CAMTEC), University of Victoria, Victoria, British Columbia V8W 2Y2, Canada

* Corresponding author E-mail address: wulff@uvic.ca

Abstract

Disulfide acids are important for traceless release mechanisms in prodrugs and drug delivery applications. Their ability to self-immolate and release cargo due to environmental stimulus is invaluable. However, complex reactivity patterns may be overlooked as assays increase in complexity or are conducted in media of increasing biological relevance. Conclusions drawn from preliminary characterization in simple phosphate buffers are often applied to *in vitro* studies in which more complex media are used (e.g. containing glucose, amino acids, FBS, and the cell surface). We developed a model disulfide incorporating a fluorogenic dye as a reporter group in order to explore the generality of the disulfide prodrug system, and used this to explore the stability of disulfide esters in various contexts of increasing complexity. We found that our reporter molecules prematurely released cargo in a series of cell-containing and cell-free assays. We systematically reverse-engineered the components of a complex cell medium and found that FBS was capable of interfering with disulfide-based prodrug linkers, triggering the release of conjugated 4-methylumbelliferone (4-MU) from representative reporter molecules. FBS consistently induced 4-MU release in complete media (i.e. DMEM and RPMI 1640), minimal essential media, and in pure water. Signs of 4-MU release were mitigated when FBS was subjected to intense heat (> 100 °C) or esterase-specific protease inhibitor cocktail (PIC), indicating that esterases from the serum were capable of triggering cargo release using a hydrolysis mechanism that is separate from the desired reductive cleavage pathway. These findings are important because they show that variance in models may hide unexpected results, which calls for more meticulous consideration of control experiments when developing stimulus-release agents for biological applications.

Keywords

Drug release, nanoparticles, disulfides, premature release, esterases, cell-culture media

Introduction

Self-immolation is frequently used in drug delivery systems to facilitate the release of a drug by controlled disassembly of the vehicle or a prodrug form.[1–14] In controlled drug delivery systems, the triggered release of a drug is attributed to intentional deconstruction of the vehicle by an external factor or stimulus, which releases the active drug moiety. Stimuli may be intrinsic environmental factors such as changes in pH or temperature, irregular concentration of redox reactive species, or external factors like light or ultrasound.[15–18]

The tumour microenvironment (TME) is reported to be more acidic and highly reductive, making it a prime target for stimulus-based drug delivery.[2–4,19–23] The irregular environment (relative to basal cell conditions) is caused by an imbalance in metabolites. One frequently associated metabolite with the TME is reduced glutathione (GSH), a common thiol-containing tripeptide; it is reported at unusually high concentrations surrounding tumours.[20] The abnormal concentration of GSH consequently introduces an immediate reducing extracellular matrix relative to healthy tissues, making it an excellent focus for stimulated release via disulfide-based prodrugs or nanoparticle release mechanisms.[5,20,24]

Disulfides are an important moiety in nanomaterials for drug delivery due to their redox capability for controlled deconstruction.[3,6,8,11,25–28] Dithiodiacids are useful as prodrug linkers with their two carboxylic acid handles for potential asymmetric conjugation, and the disulfide bridge which is reactive with a reducing environment. Upon reduction of the disulfide, the free thiol (or thiolate) is capable of nucleophilic addition to the nearby carbonyl group, resulting in the formation of a thiolactone and ultimately releasing the active drug species (Scheme 1). Disulfides are a traditional approach to redox-responsive nanocarriers selective for a reducing environment.[3,4,14,29–38] Their response to the environment may induce swelling or shedding of the hydrophilic component of a vehicle, releasing the payload into the bulk. Disulfides have also been used as chemodosimeters to discriminate various thiols.[39,40] Bohn *et al.* used a series of asymmetric disulfide–linker prodrugs to discriminate and decrease esterase degradation, effectively improving the half-life of the molecules; the increased hydrophobicity also helped the molecules cross the blood-brain barrier.[34]

In this work, we employed dithiodiacids as a means of selective and controlled release for the reducing character of the TME using turn-on fluorescence from liberated 4-MU as the primary readout. However, we found an incompatibility with common cell culturing techniques when transitioning from molecular-based studies to cellular environments. Herein we emphasize how common biological reagents were used to discriminate the stability of our compounds, and how cell culturing techniques and conditions affected our controlled release studies when transitioning into more complex systems.

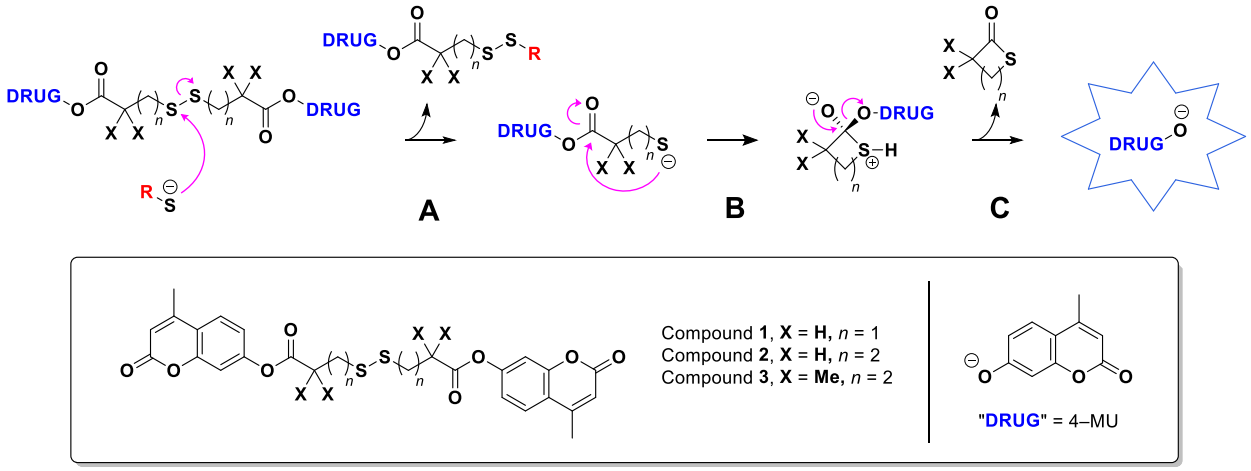

Scheme 1. General mechanism of disulfide-induced release of 4-MU anion from fluorescently quenched bis-esterified prodrugs **1**–**3**. **A**. Exchange or reduction of the disulfide with another thiolate-species is expected to form the free thiolate. **B**. The reduced thiolate undergoes an intramolecular nucleophilic substitution cyclization forming an unstable intermediate. **C**. The intermediate species collapses favouring formation of the thiolactone, which releases the drug into the bulk. 4-MU behaves as a surrogate drug with turn-on fluorescent properties when in the anionic form. The inset presents the structures of the 4-MU anionic fluorophore and the variation between traceless prodrug linkers in compounds **1**–**3**. The complete structures are shown in Figure S1.

Materials and methods

1.1. Materials:

3,3'-dithiodipropionic and 4,4'-dithiodibutyric acid, EDC, 4-MU, DMAP, DCM, MeOH, oxidized glutathione (GSSG), reduced glutathione (GSH), cysteine (Cys), *meta*-chloroperoxybenzoic acid (*m*CPBA), Na_2S, NaSH, Tris-HCl, and acetonitrile were obtained from Sigma. TCEP was obtained from ChemImpex. All culturing media (DMEM, RPMI 1640, DPBS, and MEM) were purchased from ThermoFisher, 100x Protease Inhibitor Cocktail Set I purchased from Calbiochem, and Fetal Bovine Serum (FBS) One shot was purchased from Gibco.

1.2. Instruments:

1.2.1. NMR, IR, and HRMS

^{1}H NMR spectra were either recorded at 500.27 or 300.27 MHz, respectively, on a Bruker AVANCE NEO 500 spectrometer equipped with a BBF probe or a Bruker AVANCE 300 spectrometer equipped with a 5 mm PABBO BB-1H/D Z-GRD probe. ^{13}C NMR spectra were recorded at 125.81 MHz on a Bruker AVANCE NEO 500 spectrometer equipped with a BBF probe. ^{1}H chemical shifts (δ) are reported in parts–per–million (ppm) relative to tetramethylsilane and referenced to the solvent peak ($CDCl_3$, δ 7.27). NMR data is presented as follows: chemical shift, multiplicity (s = singlet, d = doublet, dd = doublet of doublets, dt = doublet of triplets, qt = quintet, app = apparent, m = multiplet), coupling constants (J, reported in Hz), integration. All ^{13}C NMR spectra are proton-decoupled (^{13}C{1H}). ^{13}C chemical shifts (δ) are reported in parts-per-million (ppm) relative to tetramethylsilane and referenced to the solvent peak ($CDCl_3$, δ 77.2)

IR spectra were recorded using a Perkin-Elmer ATR spectrometer, and wavenumbers (ν) were reported in cm^{-1}. In addition, high-resolution electrospray ionization mass spectrometry (HRMS) data were acquired using a Thermo Scientific Orbitrap Exactive Plus spectrometer.

1.2.2. Fluorescence monitoring

All fluorescence experiments monitored release of 4-MU with fixed excitation and emission wavelengths of 315 nm and 445 nm, respectively. Any observed release of the fluorophore from compounds **1** and **2** was normalized with respect to 2 mol eq. 4-MU in the appropriate medium, expressed as a percentage described in Equation 1. The fluorescence intensity of 4-MU release in cell-free media was kinetically monitored using a SpectraMax M5 (Molecular Devices LLC, US) by reading every 180 s for compounds **1** and **2**, and every 300 s or 600 s for compound **3**. The fluorescence intensity of cell supernatant was measured using an Infinite M Nano plate reader (Tecan, Switzerland). Plates were incubated at 37 °C.

1.3. Molecular characterization

Stock solutions of prodrugs **1** and **2** were made in 100% acetonitrile and were diluted to a working concentration of 200 µM (20x) with 30% MeCN / 70% Tris buffer, pH 7.4. Two Tris buffer stocks was prepared using Tris-HCl. The first (Tris buffer A) was a working stock at 71.4 mM, such that it would have a final concentration of 50 mM when 30% (v/v) MeCN was added. Tris buffer B was prepared at 50 mM Tris-HCl and used as the solvent for preparing reagent stocks. Both Tris buffers had their pH adjusted to 7.4 with 6 M NaOH. The reagent stocks used in Figure 1 were prepared at 31.6x concentrate, such that the final concentration would be 30 mol eq. relative to the traceless linkers. In a 96-well plate, 10 µL of 20x compound solution (3:7 MeCN/Tris buffer A) was further diluted with 190 µL 31.6x reagent solution (Tris buffer B) to afford a solution containing 1x compound (10 µM), 30x of the stimulus reagent (300 µM), and 1.5% v/v MeCN in 200 µL.

The spectrophotometer detected fluorescence of 4-MU by exciting at 315 nm and detecting the emission at 450 nm. This was performed either in a quartz cuvette with a 1 cm pathlength or in a 96-well plate with a with 1 cm pathlength. The fluorescent release profile of “high” concentration acetonitrile was 5% v/v – by preparing 20x stocks of compound in acetonitrile (100% v/v) and performing 1:19 dilution with the 30 mol eq. reactive species in Tris buffer.

1.3.1.1. Cell-free plate assay

The cell-free plate assays had the molecule dissolved in the above mixture as a stock solution and diluted into the appropriate media, treated with either 30 mol eq. TCEP and/or FBS. Untreated media was used as a negative control. The plate was excited at 315 nm to stimulate emission of 445 nm light from released 4-MU. Readings were taken every five min.

1.4. Syntheses of compounds **1**–**3**

1.4.1. Synthesis of compound **1**

Compound **1** was synthesized using conventional peptide coupling, based on the work of Zou *et al*. In a round bottom flask, 235 mg of 3,3'-dithiodipropionic acid (1.1 mmol) was mixed with 2.2 mol eq. 4-methyl umbelliferone (4-MU, 430 mg), 2.2 mol eq. EDC (462 mg), and 0.3 mol eq. DMAP (43 mg) in anhydrous DCM (30 mL). The mixture was stirred for 18 h at 25 °C under inert atmosphere. The crude mixture was concentrated *in vacuo* and the product was purified using a gradient column starting at 100% DCM and slowly increasing amounts of MeOH. Prodrug **1** was isolated as a fine colorless powder at 56% yield.

^{1}H NMR δ (DCM–d_2): 2.45 (3H, s), 3.12 (4H, m), 6.26 (1H, s), 7.13 (1H, app dd, 8.3 Hz, 2.3 Hz), 7.14 (1H, app s), 7.66 (1H, d, 8.3 Hz).

^{13}C NMR δ (DCM–d_2): 18.53, 29.71, 32.86, 34.20, 110.20, 114.48, 117.89, 125.62, 152.10, 152.90, 154.17, 160.12, 169.77.

1.4.2. Synthesis of compound **2**

Compound **2** was made using similar peptide coupling conditions. In a round bottom flask, 240 mg of 3,3'-dithiodbutyric acid (1 mmol) was weighed with 2.1 mol eq. 4-MU (370 mg), 2.1 mol eq. EDC (410 mg), and 0.3 mol eq. DMAP (40 mg) in anhydrous DCM (30 mL). The mixture was stirred for 18 h at 25 °C under inert atmosphere. The crude mixture was concentrated *in vacuo*, and the product was purified using a gradient column starting at 100% DCM and slowly increasing amounts of MeOH. The isolated product had a 70% yield.

^{1}H NMR δ (DCM–d_2): 2.17 (2H, qt), 2.41 (3H, s), 2.76 (2H, t), 2.84 (2H, t), 6.22 (1H, s), 7.07 (1H, app dd), 7.10 (1H, app d), 7.62 (1H, d).

^{13}C NMR δ (DCM–d_2): 18.63, 24.11, 32.70, 37.70, 110.34, 114.50, 118.01, 118.06, 125.67, 152.26, 153.16, 154.28, 160.31, 171.05.

1.4.3. Synthesis of compound **3**

Compound **3** was from commercially available gamma-butyrolactone (GBL, Sigma) in five steps as presented in Scheme S1.

All commercial materials were used as received without any further purification. 3,3-dimethyldihydrofuran-2(3H)-one (**5**)[41], 3,3-dimethyldihydrothiophen-2(3H)-one (**6**)[42] and 4,4'-disulfanediylbis(2,2-dimethylbutanoic acid) (**7**)[43] were synthesized by the reported methods in the supplementary references.

1.4.3.1. 3,3-dimethyldihydrofuran-2(3*H*)-one (**5**)

In a flame-dried flask under argon, sodium hydride (60% in mineral oil, 5.58 g, 139 mmol) was added to tetrahydrofuran (40 mL) at 0 °C in portions. The ice bath was removed, and the suspension was stirred at room temperature for 5 min, then heated at 70 °C. At this temperature was added a solution of methyl iodide (9.0 mL, 145 mmol) and γ-butyrolactone (**4**; 4.4 mL, 58.1 mmol) in tetrahydrofuran (10 mL) over 30 min. After 3 h, the mixture was cooled to 0 °C,

quenched with saturated aqueous ammonium chloride (100 mL) and extracted with ethyl acetate (3 × 100 mL). The combined organic layers were dried over magnesium sulfate, concentrated under reduced pressure, filtered through a silica plug (2 cm), and washed with diethyl ether (150 mL). The solution was concentrated to afford 3,3-dimethyldihydrofuran-2(3*H*)-one (**5**) as a colorless oil. (5.44 g, 82%). The ATR-IR diagnostic peak was 1762 cm^{-1}.

^{1}H NMR (500 MHz, $CDCl_3$) δ 4.25 (t, *J* = 7.0 Hz, 2H), 2.10 (t, *J* = 7.0 Hz, 2H), 1.25 (s, 6H).
^{13}C NMR (126 MHz, $CDCl_3$) δ 182.37, 64.77, 38.62, 37.08, 24.21.
IR (diamond-ATR): 2971, 2933, 2875, 2255, **1762**, 1615, 145, 1389, 1367, 1263, 1230, 1203, 1167, 1103, 1027, 998, 965, 907, 755, 729 cm^{-1}.

1.4.3.2. 3,3-dimethyldihydrothiophen-2(3*H*)-one (**6**)

To a round bottom flask equipped with a condenser was added 3,3-dimethyldihydrofuran-2(3*H*)-one (**5**) (4.56 g, 40 mmol) and potassium thioacetate (7.31 g, 1.6 eq, 64 mmol) in *N*,*N*-dimethylacetamide (50 mL). The mixture was heated at 160 °C for 4 h. The reaction mixture was then cooled to room temperature, and water (150 mL) was added. The product was extracted with hexane (3 × 150 mL). The combined organic layer was washed with saturated sodium chloride and dried over magnesium sulfate. The solvent was evaporated to afford 3,3-dimethyldihydrothiophen-2(3*H*)-one (**6**) as a pale-yellow oil (3.71 g, 71 %). ATR-IR showed the diagnostic thioester peak at 1697 cm^{-1}.
^{1}H NMR (500 MHz, $CDCl_3$) δ 3.24 (t, *J* = 6.6 Hz, 2H), 2.10 (t, *J* = 6.6 Hz, 2H), 1.16 (s, 6H).
^{13}C NMR (126 MHz, $CDCl_3$) δ 213.24, 48.97, 40.28, 28.19, 23.54.
ATR-IR C=O(S), 1697 cm^{-1}

1.4.3.3. 4,4'-disulfanediylbis(2,2-dimethylbutanoic acid) (**7**)

3,3-dimethyldihydrothiophen-2(3H)-one (**6**; 2.60 g, 20 mmol) was suspended in an aqueous NaOH solution (3.20 g, 80 mmol, 4 eq, in 8 ml water), and the resulting mixture was then heated to 110 °C for 20 min in preheated oil bath. The mixture was then cooled to 0 ºC. HCl (35%, 16 mL) was added dropwise. The mixture was then extracted with diethyl ether (3 × 50 mL), dried over $MgSO_4$, and concentrated under reduced pressure.
The crude residue from the above reaction mixture was dissolved in MeOH (100 mL), NaOH (800 mg, 20 mmol) and KI (2g, 12 mmol, 0.6 eq). Iodine (2.53 g, 10 mmol, 0.5 eq) was added portion-wise and the solution was stirred for 2 h. The brown reaction mixture was decolored with a saturated sodium sulfite solution, the solvents were removed under reduced pressure, the residue was dissolved in EtOAc (100 mL) and the resulting solution was washed with aqueous HCl (1 M, 100 mL) and water (100 mL). The organic phase was dried over $MgSO_4$, filtered, and concentrated under reduced pressure. Purification of the crude material was accomplished by crystallization from Et_2O to give 4,4'-disulfanediylbis(2,2-dimethylbutanoic acid) as a white solid

(1.76 g, 59%). The diagnostic ATR-IR peaks were the broad OH stretch from 3600–2400 cm^{-1} and a strong 1689 cm^{-1} absorbance corresponding to the carbonyl stretch.

^{1}H NMR (500 MHz, $CDCl_3$) δ 2.70 – 2.61 (m, 4H), 1.99 – 1.90 (m, 4H), 1.24 (s, 12H).

^{13}C NMR (126 MHz, $CDCl_3$) δ 184.25, 42.16, 39.88, 33.90, 25.05.

HRMS (ESI-) m/z [M-H] calculated for $C_{12}H_{21}O_4S_2$: 293.0881, found: 293.0887.

1.4.3.4. bis(4-methyl-2-oxo-2H-chromen-7-yl) 4,4'-disulfanediylbis(2,2-dimethylbutanoate) (**3**)

4,4'-disulfanediylbis(2,2-dimethylbutanoic acid) (**7**) (294.1 mg, 1.0 mmol), 4-dimethylaminopyridine (DMAP, 122.2 mg, 0.6 mmol), 1-(3-dimethylaminopropyl)-3-ethylcarbodiimidehydrochloride (EDC, 575.1 mg, 3 mmol) and 7-hydroxy-4-methylcoumarin **(5)** (387.3 mg, 2.2 mmol) were mixed in 20 mL of anhydrous dichloromethane. The mixture was stirred at room temperature 24 h and then at 40 °C for another 24 h. The mixture was then cooled to room temperature and the solvent was removed under reduced pressure. The resulting residue was purified by silica gel column chromatography using a gradient of 1:2 pentane:dichloromethane to pure dichloromethane to yield the target compound **6** as an off-white solid (416.2 mg, 68 %).

^{1}H NMR (500 MHz, $CDCl_3$) δ 7.56 (d, *J* = 8.6 Hz, 2H), 7.06 (d, *J* = 2.3 Hz, 2H), 7.01 (dd, *J* = 8.6, 2.3 Hz, 2H), 6.24 (d, *J* = 1.4 Hz, 2H), 2.76 – 2.71 (m, 4H), 2.41 (s, 6H), 2.12 – 2.07 (m, 4H), 1.36 (s, 12H).

^{13}C NMR (126 MHz, $CDCl_3$) δ 175.07, 160.42, 154.12, 153.32, 151.97, 125.44, 117.98, 117.77, 114.48, 114.47, 110.30, 42.67, 40.12, 34.33, 25.05, 18.71.

IR (diamond-ATR): 3067, 2972, 2925, 1750, 1722, 1706, 1626, 1614, 1570, 1499, 1474, 1459, 1388, 1369, 1330, 1255, 1193, 1129, 1095, 1066, 1037, 1017, 983, 915, 883, 861, 7990, 750, 738 cm^{-1}.

HRMS (ESI+) m/z [M+Na] calculated for $C_{32}H_{34}O_8S_2Na$: 633.1592, found: 633.1587.

1.5. Molecular characterization:

1.5.1. Fluorescence spectroscopy

A SpectraMax M5 plate reader was used to monitor release of 4-MU. Measurements were made using 96-well flat-bottom plates (Corning Costar). 4-MU was excited at 315 nm, and emission was measured at 450 nm. Upon conjugation, the emission peak of the coumarin was suppressed, but this quenching was shown to be reversible upon addition of at least 30 mol eq. TCEP. Time-dependent release of 4-MU from the model prodrugs was normalized relative to the intensity of 2 mol eq. free 4-MU using equation 1 as described below:

$$Release\ (t) = \frac{F(t)-F_0}{F_{4-MU}-F_0} * 100\% \quad (1)$$

where "*Release (t)*" is the normalized release represented as a percentage, "*F(t)*" is the observed fluorescence at a given time point, "F_0" is fluorescence intensity of media, and

"$F_{4\text{-}MU}$" is the intensity of the total 4-MU (2 mol eq. relative to the traceless linker). Time was set to 0 s when the prodrugs were added to their respective well.

1.5.2. Turn-on fluorescence of fluorogenic reporter compounds

Compounds **1** and **2** were screened for selective turn-on fluorescence with reducing agents, oxidizing agents, and sulfur exchanging species (Figure 1, Figure S3, Figure S4). In a 96-well plate, 10 µM of the test compound was treated with 30 mol eq. TCEP, glutathione (GSH), oxidized glutathione (GSSG), cysteine (Cys), H_2O_2, or *m*CPBA and monitored for 4-MU release with the previous conditions.

Compounds **2** and **3** were screened for selective turn-on fluorescence as described above (Figure S5).

1.6. Cell-based studies

1.6.1. *In vitro* culture of U-87, U-251, and HNDF cells

Human-derived glioma cell lines, U-87 (ATCC® HTB–14™) U-251 (Creative Bioarray, CSC–6321W) and human primary normal dermal fibroblast cells (ATCC® PCS-201-212^{TM}) were cultured according to the standard protocol provided by the supplier. Briefly, cells (of passage 3–8) were initially grown in a Corning 25 cm² Rectangular Canted Neck Cell Culture Flask using Dulbecco's modified Eagle's medium (DMEM, Gibco™ by Life Technologies™, USA) treated with 10% FBS (Gibco™ by Life Technologies™, USA) and 1% penicillin-streptomycin (10,000 unit/mL, Gibco™ by Life Technologies™, USA) as the growth medium. Cells were incubated in an atmosphere of 5 % CO_2 at 37 °C.

When cells were 85% confluent, they were detached from the surface of culture flask when growth media was replaced with 3 mL trypsin-EDTA (Gibco™ by Life Technologies™, USA) and incubated at 37 °C for 5 min. Following this step, 6 mL of growth media was added to the detached cells to deactivate trypsin activity, followed by centrifuging the cell suspension at 300xG to make a cell pellet. The supernatant was discarded, and 1 mL of fresh growth media was added to the cell pellet to suspend the cells by gentle pipetting.

The next step was seeding cells in Corning 96-well plate at the density of 3000 cells/well and incubating the well plate at 37 °C in an atmosphere of 5 % CO_2. After 24 h, the cell culture media in each well was replaced by 300 µL of prodrug solution (10 and 20 µM of compound **1** or **2** dissolved in growth medium) and incubation was maintained for 24 h. A control solution of free 4-MU was prepared to monitor "full" release (20 and 40 µM, respectively).

1.6.2. Compound **1** release study with U-87 glioma cells

U-87 cells were seeded in a 96-well plate at a density of 3000 cells/well as described above. After 24 h the cell growth media was replaced with 300 µL of different release media. To obtain different release media containing 10 µM of compound **1**, a stock series was diluted in several media such as DPBS, DPBS+Glucose, DPBS+Glucose+Glutamine, and

DPBS+Glucose+Glutamine+FBS. The concentrations of glucose, glutamine, and FBS were 4.5 g/L, 0.584 g/L, and 10% (v/v), respectively. Also, the standard release medium was prepared by dissolving equivalent concentration of 4-MU (20 µM) in the same series of buffers. After 24 h, cell media was removed and replaced with appropriate release medium and standard release medium. At predetermined time points, the fluorescence intensity was measured as described before and the obtained intensity was normalized with respect to the intensity of the equivalent concentration of 4-MU cultured in the same release medium. The experiment was carried out with 6 replicates.

1.6.3. Cell viability assay

To identify the effect of release media and compound **1** on the cell viability, U-87 cells were seeded in a Corning 96-well plate at a density of 3000 cells/well as previously described. After 24 h, the cell media was removed and replaced with different release media containing 10 µM compound **1**. Cells cultured with cell media and Milli-Q water were considered as the positive and negative controls, respectively. At specific time points (namely 12 h, 24 h, 48 h, and 72 h), the release media was removed and replaced with 110 µL of cell media containing 10% (v/v) PrestoBlue reagent (Invitrogen, USA). After 30 min of incubation at 37 °C, 100 µL of supernatant was taken from each well and the fluorescent intensity of supernatant was measured using an excitation wavelength of 560 nm and emission wavelength of 590 nm. The results were normalized with respect to the positive control to obtain relative viability. The experiment was carried out with 6 replicates.

1.7. Cell-free thiol release assays

Fluorescent release from model prodrug compounds was followed in a 96-well plate, under various conditions with various media to assess what was causing reduction of the disulfide linker. Any turn-on fluorescence observed from either compound was normalized to a control series of wells with 2 mol eq. 4-MU. Each subsequent experiment contained a background series of simply media absent of compounds **1** and **2** or 4-MU. The plate was monitored for turn-on fluorescence every 5 min, for a duration of 1 h, using the same excitation and emission wavelengths described above. The media investigated were DMEM, RPMI 1640, MEM, and MilliQ water. Each sample replicate was measured from at least three wells.

A final assay was performed using MilliQ water alone treated with or without 10% FBS. With a fresh FBS shot, the serum was either heat-treated at >110 °C for at least 1 h in a water bath prior to mixing with MilliQ water or treated normally by incubating at 37 °C. To determine if there was esterase activity, an additional 1% PIC was also added. The plate was assayed under the same conditions as above: monitoring turn-on fluorescence of 4-MU from the prodrugs, where the intensity was normalized to 2 mol eq. of 4-MU, reading the emission wavelength at 445 nm every 5 min for 1 h.

Time-dependent analysis was performed using one-way ANOVA between at least three replicates, comparing averaged intensity at the initial time for the experiment with averaged intensity at 1 h. This was done to determine if background hydrolysis of 4-MU was significant in buffer control, and to determine the effects of the reagents after 1h of incubation.

Time-independent analysis was performed using two-way ANOVA between at least three replicates, comparing averaged intensity at 1 h between reagents. This test allowed us to compare intensities induced by reagent to background hydrolysis.

Results and discussion

Compound synthesis and screening of 4-MU release

Compounds **1** and **2** were synthesized as models of selective payload release for the tumour microenvironment, by turn-on fluorescence of the conjugated fluorophore 4-methylumbelliferone (4-MU; Scheme 1). The fluorescence of 4-MU is quenched when the dye is esterified through the phenol group (Figure S2). Previously, Zou *et al*. reported compound **1** as a chemodosimeter for endogenous H_2S.[39] Zou's findings suggested that H_2S exchanges with the disulfide, forming an asymmetric nucleophilic persulfide, which causes release of one 4-MU molecule. Zhang *et al*. noted a similar mechanism with benzodithiolane released alongside the liberated fluorophore.[40]

The two reporter molecules (at 10 µM) were first screened for reactivity with various biologically relevant oxidizing and reducing agents (30 molar equivalents; i.e. 300 µM) in Tris buffer containing 1.5% v/v acetonitrile (MeCN). The concentration of stimulant was selected to match the previous studies by Zou,[39] and to be consistent with the expected concentration of GSH in biologically relevant tissue.[44,45] The emission intensity observed from each experiment was normalized to that of 2 molar equivalents of free 4-MU. In buffer alone, a low rate of background hydrolysis was observed, such that <5% release of 4-MU occurred from **1** or **2** within the first hour of incubation (Figure 1), while approximately 15% release of 4-MU was observed following a 24 h incubation (Figures S3–S4). To confirm that disulfide reduction was capable of initiating 4-MU release, we employed a non-thiol-containing reducing agent, *tris*-carboxyethyl phosphine (TCEP), as a positive control.[46,47] As expected, TCEP triggered significant 4-MU release from both **1** and **2** within 1 h ($P < 0.0001$; Figure 1 and Table S1).

Thiol-containing biological reducing agents, glutathione (GSH) and cysteine (Cys), were similarly effective at triggering 4-MU release from compound **1**, leading to a statistically significant increase in fluorescence within 1 h ($P < 0.0001$; Figure 1A and Table S1). In both cases the rate of 4-MU production was significantly larger than that of background hydrolysis ($P = 0.024$ for GSH; $P < 0.001$ for Cys; Table S2). As expected, a negative control molecule that lacks free thiol groups (glutathione disulfide; GSSG) did not lead to a significantly greater release of 4-MU than was observed in the buffer-only samples ($P = 0.92$; Table S2).[48]

Interestingly, the oxidants hydrogen peroxide (H_2O_2), potassium peroxymonosulfate (Oxone), and *meta*-chloroperbenzoic acid (*m*CPBA) were also effective at liberating 4-MU from compound **1** within 1 h ($P < 0.0001$ for each oxidant; Figure 1A and Table S1). For H_2O_2 in particular, the rate of production of 4-MU was significantly greater than that observed in the buffer-only samples ($P < 0.0001$; Table S2). Indeed, H_2O_2 induced a greater degree of 4-MU production than did glutathione, cysteine, or even TCEP. This is an intriguing result given that disulfides (including dithiodiester motifs) are often assumed to be predominantly sensitive to *reductive* cleavage conditions—although oxidative cleavage has also been well described in the literature.[49] Clearly their equivalent sensitivity to oxidative conditions is important to bear in mind when designing drug-releasing small-molecule or nanoparticle constructs.

Compound **2** was likewise found to be sensitive to the positive control molecule (TCEP) and to be insensitive to the negative control molecule (GSSG). In the case of TCEP, a statistically significant production of 4-MU was observed from **2** within 1 h ($P < 0.0001$; Figure 1B and Table S1), and this rate of increase in fluorescence was significantly greater than that observed in the buffer-only vehicle control samples ($P < 0.0001$; Table S2). In the case of GSSG, no significant increase in fluorescence was observed, relative to that of the vehicle control samples ($P = 0.42$; Table S2).

Interestingly, however, compound **2** was generally less sensitive to the presence of either oxidants or reducing agents. Within 1 h, cysteine triggered no statistically significant release of 4-MU relative to the rate of background hydrolysis ($P = 0.88$; Table S2), while the rate of GSH-triggered 4-MU production was modest ($P = 0.0034$ after 1 h; Table S1) and was not statistically significant when compared to the rate of hydrolysis in the vehicle control samples ($P = 0.19$; Table S2). Intriguingly, H_2O_2 was the only agent tested (other than the TCEP positive control) which led to a rate of 4-MU production from compound **2** that exceeded that of background hydrolysis to a statistically significant degree ($P = 0.022$; Table S2). This once again reinforces the need to consider *oxidative* release mechanisms for disulfide systems alongside reductive mechanisms. At the same time, it must be recognized that hydrogen peroxide can promote ester hydrolysis as well as disulfide oxidation; this alternative mechanism of 4-MU liberation is discussed in more detail below.

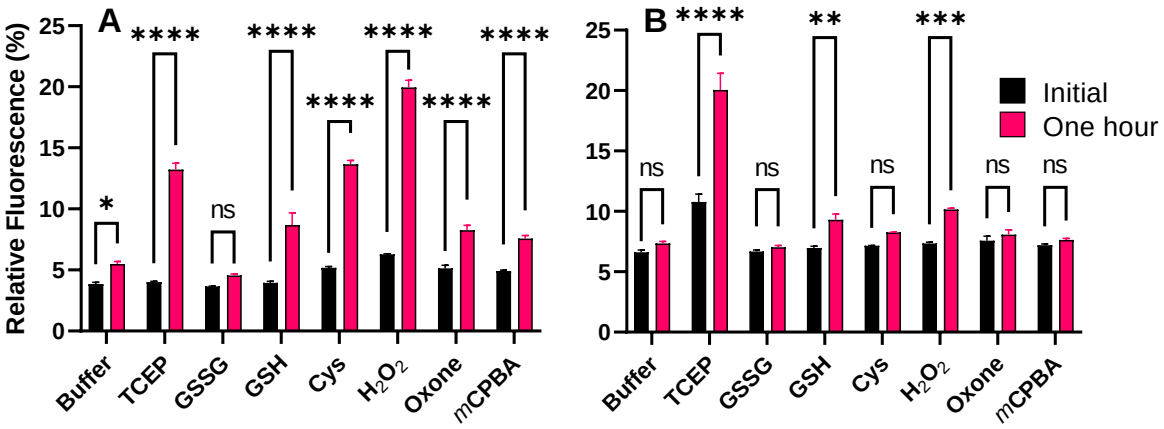

Figure 1. Compounds **1** (**A**) or **2** (**B**) at 10 µM were monitored for reactivity with 30 mol eq. (300 µM) of various reducing and oxidizing agents by a means of turn-on fluorescence from liberated 4-MU in Tris buffer containing 1.5% MeCN. A two-way ANOVA analysis was used between 4 replicates to compare intensities between time points, and a one-way ANOVA analysis was used to investigate time-dependent release. The bars represent standard error of mean (SEM) (* : $P < 0.05$, ** : $P < 0.01$, *** : 0.001, #: $P < 0.0001$). The complete statistical comparison is shown in Table S1. Data from longer incubation times (24 h) are shown in Figure S3 and Figure S4 for compounds **1** and **2**, respectively.

When the release reaction was allowed to proceed for 24 h (Figures S3–S4), a further increase in 4-MU production was observed from compounds **1** and **2** in the positive control experiments that used TCEP as the reducing agent (up to *ca.* 50% conversion in both cases), while the negative controls using GSSG once again showed no greater amount of 4-MU production than was found in the vehicle control samples. In the 24 h measurement, cysteine, hydrogen peroxide, Oxone and *m*CPBA all elicited a statistically greater amount of 4-MU release than was observed in the vehicle control samples (Table S3), while for compound **2** only hydrogen peroxide triggered 4-MU release at a rate that was higher than that of background hydrolysis.

Bohn *et al.* reported that increased hydrophobicity in the disulfide-containing reagent corresponded to a slower rate of reduction.[34] This observation was consistent with our finding that compound **2** appeared to react less efficiently with both oxidants and reducing agents than did compound **1**, but we wondered whether the reason behind the reduced reactivity was due to decreased solubility (or increased aggregation) for the marginally more lipophilic **2**, or whether it might simply be due to differences in the rate of attack of the thiol (or thiolate) nucleophile at the electrophilic carbonyl group (Scheme 1), given that the aliphatic linkers in **1** and **2** were of different lengths, and thus may engage in cyclization (to make 4- and 5-membered thiolactones) at different rates. Alternatively, it is possible that direct thiolysis may play a role in 4-MU release from either or both reporter molecules. To probe whether solubility was a factor, we repeated the 4-MU release experiments using an increased concentration of acetonitrile in the Tris buffer (5% instead of 1.5%).

No differences were observed in the UV/Vis spectra of **1** and **2** when the concentration of acetonitrile was increased (Figure S2), and the production of 4-MU from compound **2** remained slower than the release observed from compound **1**, no matter which chemical trigger was employed (Figure S6). We therefore conclude that aggregation likely does not play a role in the reduced reactivity of **2**, and that instead the reduced rate of production of 4-MU from this reporter reagent was either due to the intrinsic lipophilicity of the compound itself (as suggested by Bohn) or was due to differences in the release rate that stem from the use of the longer linker group.

Inadequate selectivity between different cell types

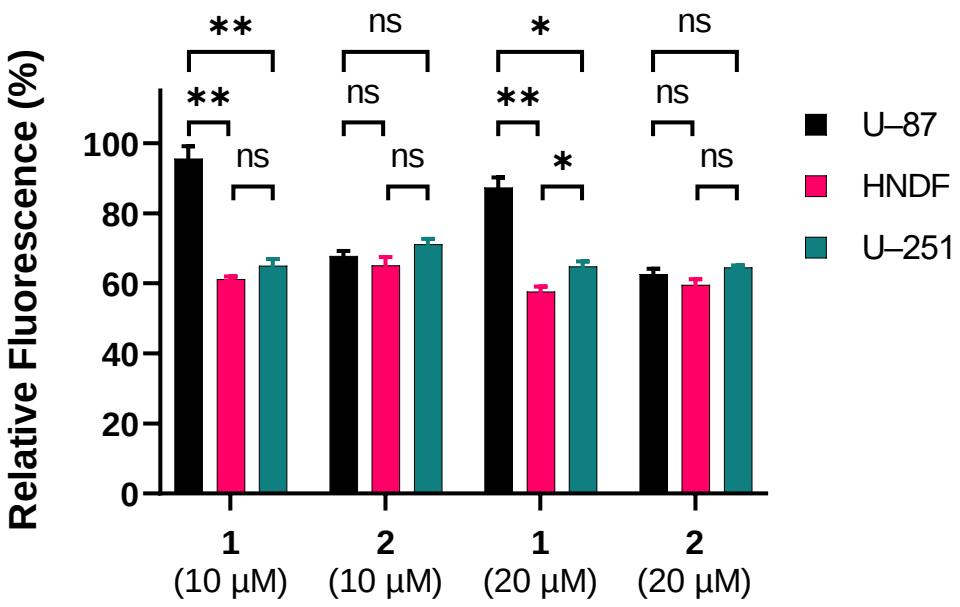

Figure 2. Compounds **1** and **2** were incubated at either 10 µM or 20 µM with human glioblastoma cells (U-87, U-251) and normal dermal fibroblasts (HNDF) to validate TME selectivity, and we poor selectivity for the release of 4-MU. The cells were treated under typical growth conditions, incubating 24 h in DMEM treated with 10% FBS at 37 °C. The fluorescence intensity was normalized to that of 2 mol eq. free 4-MU. The bars represent SEM, and n = 3. The complete statistical analysis is shown in Table S6.

Following the above confirmation that GSH was capable of inducing 4-MU release from our traceless linkers, we wanted to investigate how the compounds **1** and **2** would react when presented with varied endogenous levels of the metabolite, in the context of a cellular model system (Figure 2). From previous reports, U-87 glioblastomas have consistently higher levels of GSH than do U-251 cells, and these empirical data were used as the baseline for selectivity.[50–53] Human normal dermal fibroblasts (HNDF) cells were used as a negative control.

GSH-positive U-87 glioblastoma cells promoted a significant release of 4-MU from compound **1**, relative to both HNDF and U-251 ($P < 0.01$, Table S6). When the concentration of compound **1**

was doubled to 20 µM, the intensity of 4-MU fluorescence remained constant in U-87 and HNDF cells, whereas only at 20 µM did compound **1** display significant release of 4-MU in U-251 compared to HNDF ($P < 0.05$, Table S6). Consistent with the data from our molecular assay, which showed that **2** was less sensitive to GSH-triggered immolation than **1**, 4-MU release from compound **2** was not affected by cell type.

The above data indicated some degree of correlation between the cell-based experiment and the earlier release assays performed in Tris buffer. While we did not explicitly probe whether **1** and **2** were able to penetrate into the cells, compound **1** proved once again to be a superior reporter to compound **2**, and a modest selectivity for release by the GSH-rich U-87 glioblastoma cells was observed. At high concentrations of **1**, a greater degree of 4-MU release was observed in the second tumor cell (U-251) than in the healthy control cells, which again was consistent with the expectation that **1** may be subject to some degree of selective GSH-triggered release either inside, or—more likely—on the surface of the cells. By far the most striking observation, however, was the very large rate of background 4-MU release observed in the cell-based experiment: regardless of the cell type, >50% of the reporter dye was liberated within 24 h. This was a surprising result, given the frequency with which disulfides are employed in controlled release systems using cytotoxic payloads.[1,3,7,12,54]

We tested cell viability to determine that the emission observed was not caused by cell death (Figure S7), since it is known that 4-MU possesses modest anticancer properties, and there was a concern that apoptosis may have contributed to further release.[55] However, upon starving the cells for up to 3 days to compare the viability in the presence of the compounds, we found that the concentrations of either compound had no significant effect on cell viability (Figure S7), and the total amount of cell death was low, in both the starved control cells and in cells to which test compound had been added. This led us to believe there was something in the culturing media or culturing conditions that were causing release rather than the cells alone.

The data collected in Figure 2 suggest the linkers are not stable in complex matrices, since all cell types caused 4-MU release. However, our initial characterization (Figure 1) had been performed in a much simpler model. To probe whether the effects were induced by the cells or by some other factor in the media itself, we monitored the emission intensity of 4-MU from compound **1** with U-87 cells in a simple salt solution, Dulbecco's phosphate-based saline (DPBS), and added components that are commonly found in a complete medium (e.g. DMEM) to determine if they were contributing to the unwarranted release. We monitored 4-MU production for up to 2 h in the presence or absence of U-87 cells to isolate which of the major components could be causing the unwarranted release of the fluorophore (Figure 3). By incubating compound **1** and U-87 cells in un-supplemented DBPS, we saw that the cells did have a significant impact on 4-MU release from the traceless linker (Figure 3A), presumably as a result of disulfide cleavage. When glucose or glutamine were added to the media there was no change in intensity, unless U-87 cells were present (Figures 3B and 3C). The concentrations of the additives were comparable to what are found in the formulation of the complete medium, DMEM, at 4.5 g/L glucose and 0.5

g/L glutamine, respectively. Since the glucose and glutamine did not elicit higher intensities of 4-MU emission than in Figure 3A, they were not contributing to 4-MU liberation.

However, when 10% v/v fetal bovine serum (FBS) was added to the media there was a substantial increase in 4-MU release over 2 h, even without any U-87 cells present (Figure 3D). This FBS-promoted release was much faster than the rate of cell-promoted release observed in panels A–C. As such, no statistically significant differences could be observed in the rate of reaction in the presence vs. absence of cells, when FBS was present. When the cells were incubated for 3 days, a similar pattern of emission intensity was observed (Figure S8). Once again, when FBS was present there was no significant difference in fluorescence intensity caused by the presence of cells (Figure S8D). Interestingly, the total fluorescence emission from the released 4-MU reporter observed in DPBS supplemented with FBS (with or without U-87 cells; Figure 3D) was similar to that observed in the cell-culturing experiments described in Figure 2. These data clearly implicate fetal bovine serum as the factor contributing to premature release of the molecular cargo — a surprising result given the ubiquity of FBS in tissue culture work.

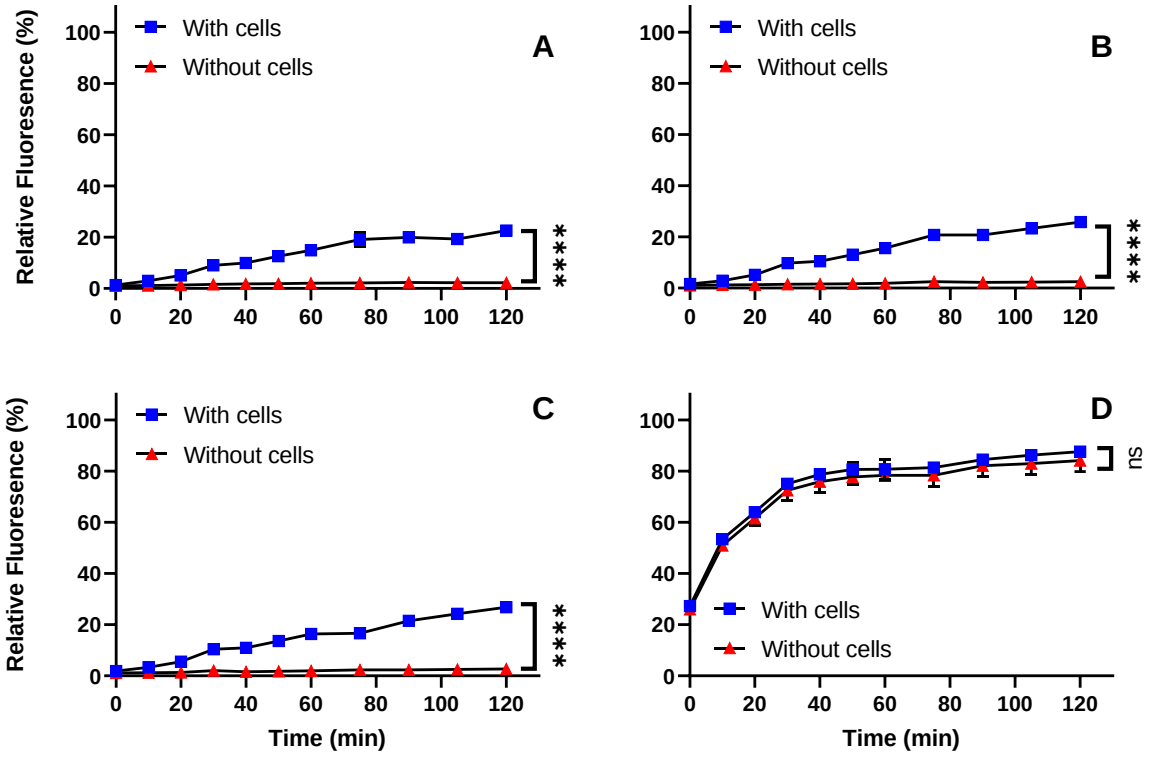

Figure 3. Compound **1** showed significant release from U-87 glioma cells within 2 h, except when media was supplemented with FBS. **A**. The traceless disulfide linker **1** was incubated with or without U-87 glioma cells in pure DPBS. **B**. The DPBS was supplemented with 4.5 g/L glucose. **C**. The DPBS was supplemented with 4.5 g/L glucose and 0.5 g/L glutamine. **D**. The DPBS was supplemented with 10% FBS (v/v) in addition to glucose and glutamine. Error

bars represent SEM of three replicates and statistics were measured at the 2 h timepoint. Compound intensity was normalized to 2 mol eq. 4-MU, expressed as a percentage. The full statistical analysis can be found in Table S8.

Next, the U-87 cells were removed to isolate how the components in the actual complete media, DMEM, could affect the traceless disulfide linkers (Figure 4). The DMEM was supplemented in one of three ways: either with TCEP (30 mol eq.) to confirm disulfide reduction and 4-MU release, or with 10% v/v FBS (a common supplement added to complex media), or with both. In all cases, significant release of 4-MU from compound **1** was observed when comparing time points at zero min and 1 h; some of this release could be attributed to background hydrolysis, as seen in the black trace. Compound **2** displayed a similar trend, except that the rate of background release in native DMEM was reduced, possibly due to a greater degree of hydrophobicity present in compound **2** vs. compound **1**. Regardless, the presence of TCEP and/or FBS had a significant impact on the release of 4-MU from both traceless linkers after 1 h, and the intensities were significantly higher than observed from background hydrolysis in DMEM (Table S9). When performed again in another complete media, RPMI 1640, we saw a similar trend in release intensity, where FBS had a significant effect of 4-MU emission (Figure S9). Interestingly, when either compound was incubated with both FBS and TCEP, there was no increase in emission intensity compared to the individual reagents alone.

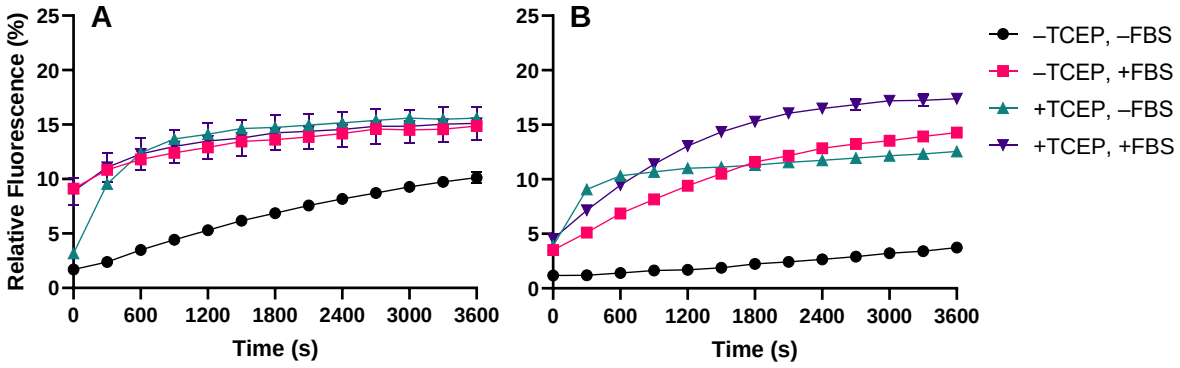

Figure 4. The release of 4-MU was monitored from traceless disulfide linker **1** (**A**) or **2** (**B**) in DMEM over 1 h. Wells were treated with either 30 mol eq. TCEP (green), 10% FBS (pink), or Both (purple). Compounds in DMEM alone were used as a control to assess background hydrolysis (black). Intensities are normalized to 2 mol eq. 4-MU and the bars represent SEM and n = 3. Error bars are present for all data points, but in some cases are two small to be resolved above and below the data marker. The complete statistical analysis is shown in Table S9.

To offset the possible effects of cysteine found in complete media affecting release of 4-MU and to focus more on the FBS-induced release, we repeated the measurements in minimum essential media (MEM) (Figure S10). In these experiments, we observed a noticeable decrease in emission intensity in the untreated MEM (black trace), relative to the previous complete media. MEM is expected to have around half the concentration of Cys, relative to DMEM and RPMI 1640.[56–58] Therefore, the decrease in intensity could be attributed to the reduced thiol content. For both compounds **1** and **2**, FBS additives still induce significant release

of 4-MU relative to untreated media ($P < 0.0001$), meaning that thiol-exchange was not a major source of unwarranted release. The same pattern was observed when MilliQ water was used as the media (Figure S11).

Assessing if the release is enzymatic and mitigated by denaturation

FBS is an essential additive for preparing complete media to sustain cellular growth.[59,60] However, it is a complex serum on its own, with growth factors and other proteins.[60,61] Therefore we wanted to assess if the serum effects were enzymatic and if they may be mitigated by denaturation and inhibitors.[59–61] To this end, we explored the effect of thermal denaturation of serum proteins (by incubation at 100 °C for 60 min) and also incorporated a protease inhibitor cocktail (PIC) using aprotinin, to deter any esterase activity on compounds **1** and **2** (Figure 5).

As anticipated by the experiments described above, the addition of FBS to a solution of compound **1** in water led to a significant release of 4-MU within 1 h (Figure 5A; $P < 0.0001$, Table S13). Addition of 1% PIC did not immediately affect the release rate, but when the FBS was thermally denatured prior to addition, the rate of 4-MU production was significantly reduced (Figure 5A, red vs. purple; $P < 0.01$). Combining the two treatments (i.e. adding 1% PIC to thermally denatured FBS) reduced the rate of 4-MU release still further (Figure 5A, purple vs. violet; $P < 0.01$).

Compound **2** showed a similar pattern to compound **1** with respect to 4-MU release, albeit with a smaller difference in emission intensity between the test samples and vehicle control (Figure 5B). When incubated with 37 °C FBS, with or without PIC, there was a significant increase in 4-MU production, compared to the background control (Figure 5B, red vs. black, green vs. black; $P < 0.0001$, Table S13). Once again, however, thermal denaturation of the FBS reduced the amount of release, and addition of PIC to the denatured serum further reduced the amount of 4-MU production. Together, these data indicate that the premature release of the 4-MU reporter group that was observed in the earlier experiments is likely to be due to esterase activity rather than disulfide reduction (Scheme 2).

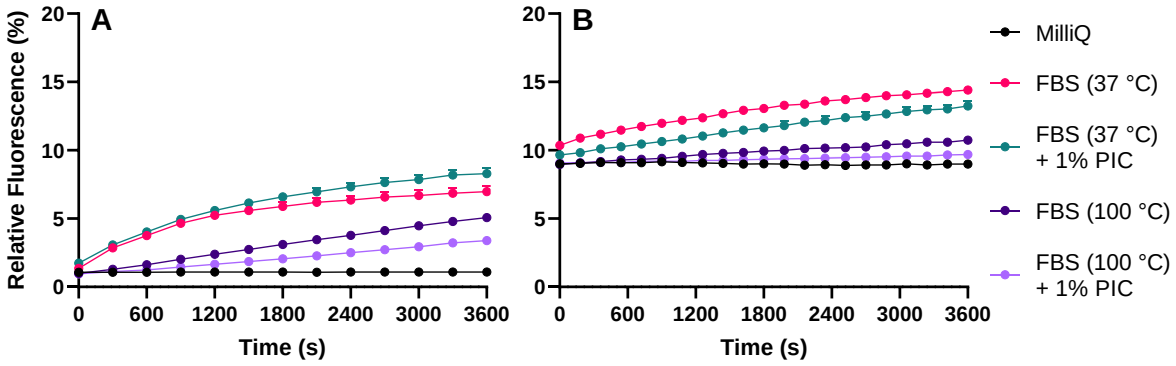

Figure 5. The enzymatic effects causing the release of 4-MU from compounds **1** (**A**) or **2** (**B**) were mitigated by denaturing FBS and incorporating a protease inhibitor cocktail (PIC) in water. FBS was treated normally by incubating at 37 °C (Pink), FBS treated with PIC (Green), FBS subjected to >100 °C without PIC (Purple) or with PIC (Violet). Error bars are SEM of n = 3. The complete statistical analysis is shown in Table S13.

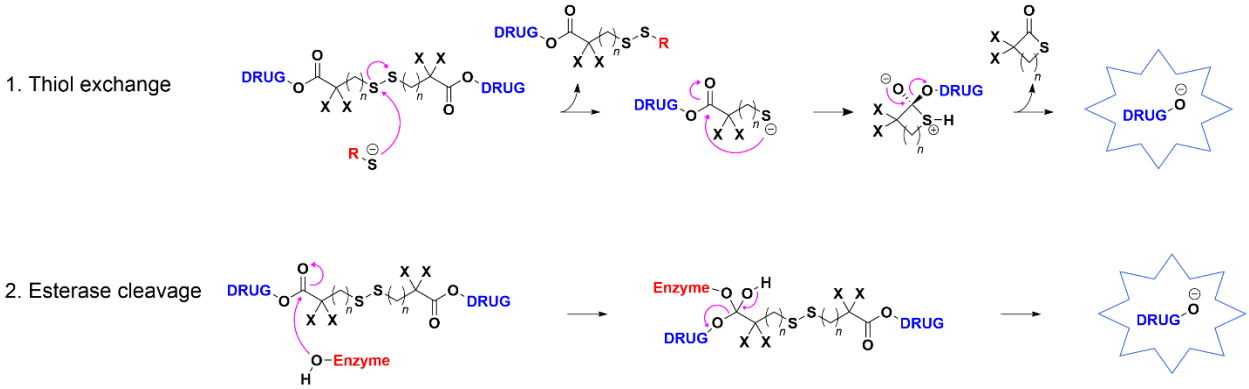

Scheme 2. Two competing mechanisms of cargo release from functionalized dithiodiacid framewoks. The fact that FBS-promoted release of 4-MU from compounds **1** and **2** can be blocked by thermal denaturation and by the use of a protease inhibitor cocktail indicates that esterase-mediated hydrolysis is dominant. To reduce the susceptibility of the reporter molecule toward esterase activity, additional steric bulk can be added adjacent to the carbonyl group.

To further prove the hypothesis that premature cargo release from **1** and **2** was due to esterase activity, and to demonstrate a ready solution to the problem of premature liberation of the active agent from disulfide diacid drug-releasing constructs, we designed and synthesized compound **3**, which incorporated two methyl groups adjacent to each carbonyl group (Figure S1, Figure 6). Inspired by previous studies from Bohn *et al.*,[34] the addition of extra steric bulk at this position was expected to disfavour enzymatic cleavage reactions.

As expected, compound **3** liberated 4-MU when treated with TCEP (employed as a positive control reducing agent; Figure S5) and did not release 4-MU when treated with GSSG (employed as a negative control). A statistically significant increase in 4-MU release (relative to background hydrolysis) was observed when **3** was treated with GSH ($P = 0.0091$) or H_2O_2 ($P = 0.0067$) for 1 h

(Table S2). Consistent with the earlier point that increased hydrophobicity appeared to reduce the rate of reaction, the average rate of 4-MU production from **3** was less than that observed for **1** or **2** (Figure S3–S5). Nevertheless, when the incubation time was increased to 24 h, we observed statistically significant 4-MU release (relative to the rate of background hydrolysis) promoted by TCEP, GSH, Cys, and H_2O_2 ($P < 0.0001$ for all four compounds; Table S3). Once again, the use of a higher concentration of acetonitrile (5% instead of 1.5%, Figure S6) did not significantly alter the emission intensity, suggesting that solubility was not a limiting factor for compound **3**.

Most importantly, we found that compound **3** had greatly improved stability in FBS-treated media, such that only very minimal hydrolysis was observed when non-denatured serum was added to a solution of **3** in water (Figure 6A). As expected, this minimal rate of hydrolysis could be further reduced by denaturing the FBS or by adding a protease inhibitor cocktail, or both (Figure 6B). These data indicate that while the addition of methyl groups adjacent to the ester groups in **3** did not completely block esterase activity, it did substantially protect the compound from unwanted enzymatic cleavage.

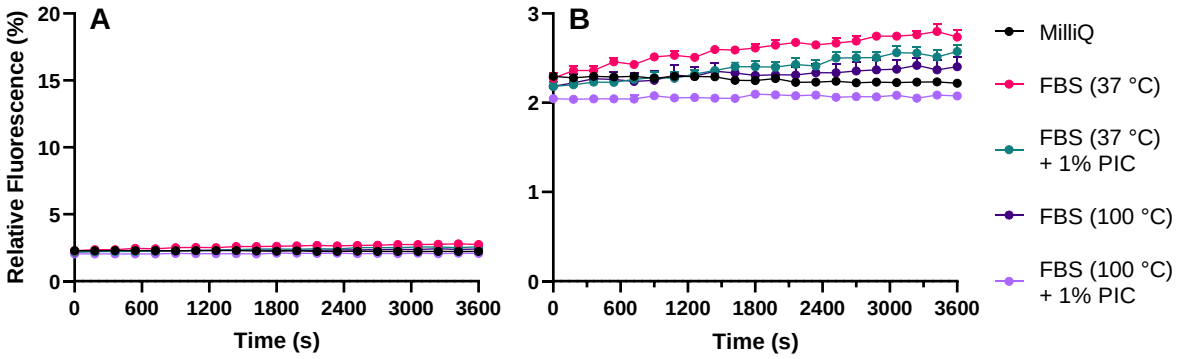

Figure 6. Compound **3** suffers substantially less FBS-promoted enzymatic cleavage, as a result of the incorporation of addition steric bulk near the carbonyl groups. Panel (**A**) shows the data on the same scale as that used for Figure 5. Panel (**B**) uses an expanded Y-axis to display the decrease in 4-MU intensities between treatments. Error bars are SEM, $n = 4$. The complete statistical analysis is shown in Table S13.

Conclusions

Traceless disulfide linkers are valuable for controlled release studies, but must be appropriately characterized prior to use in *in vitro* experiments. Upon systemic removal of the complex variables between cellular studies and our initial reducing agent screen, which had been conducted in a simple buffer matrix, we found that the common, but necessary, tissue culture additive, FBS, was a major factor in premature release of our 4-MU reporter from our disulfide constructs. When the serum was denatured by thermal treatment to inactivate enzymatic components, there was a significant decrease in release rate, and when PIC was added, the rate further decreased indicating that the cleavage observed was most likely enzyme-induced

cleavage at the ester rather than the reduced disulfide immolation (Scheme 2). This competitive (and largely undesirable) enzymatic release pathway could be almost completely blocked through the addition of extra steric bulk at the position adjacent to the ester groups that were used to conjugate the reporter molecule to the disulfide.

The use of FBS (or a similar serum additive) is a requirement for most tissue culture protocols. Moreover, all animal studies (including clinical administration of therapeutics to human patients) will necessarily involve exposing the agents under study to enzymes (including esterases) that are naturally present in circulation or within tissue. The present study shows that typical disulfide diacid constructs are much more sensitive to endogenous hydrolase enzymes than might be predicted based upon a survey of the literature, which finds these types of linkages to be used in a broad array of applications. As such, we strongly recommend that release studies be carried out using at least 10% of non-denatured FBS (rather than simply using PBS or Tris buffers, which has been the norm). Moreover, we recommend that investigators consider installing quaternary centres beside the carbonyl group that links the 'cargo' to the disulfide motif. Doing so should provide improved selectivity for triggered release over background hydrolysis.

Author credit statement

Derek Blevins: methodology, investigation, data curation, writing; original draft preparation. Rashid Nazir: methodology, investigation. Hossein Dabiri: methodology, investigation. Mohsen Akbari: supervision, funding acquisition. Jeremy Wulff: supervision, funding acquisition, conceptualization, writing; review & editing.

Declaration of competing interest

The authors declare no conflict of interest.

Data availability

Data will be made available upon request.

Acknowledgements

The authors thank the Polymer Nanoparticles for Drug Delivery (POND) CREATE program for a stipend to D.J.B., and the University of Victoria for partial operating support that was used to offset the cost of this research. We also thank the Natural Sciences and Engineering Research Council of Canada (NSERC) for operating funds.

Appendix A. Supplementary data

Supplementary data to this article can be found online at http://dx.doi.org/xxxx.

References

[1] Z. Xu, D. Wang, S. Xu, X. Liu, X. Zhang, H. Zhang, Preparation of a camptothecin prodrug with glutathione-responsive disulfide linker for anticancer drug delivery, Chem. - An Asian J. 9 (2014) 199–205. https://doi.org/10.1002/asia.201301030.

[2] G. Saito, J.A. Swanson, K.D. Lee, Drug delivery strategy utilizing conjugation via reversible disulfide linkages: Role and site of cellular reducing activities, Adv. Drug Deliv. Rev. 55 (2003) 199–215. https://doi.org/10.1016/S0169-409X(02)00179-5.

[3] C. Xu, R.J. Song, P. Lu, J.C. Chen, Y.Q. Zhou, G. Shen, M.J. Jiang, W. Zhang, pH-triggered charge-reversal and redox-sensitive drug-release polymer micelles codeliver doxorubicin and triptolide for prostate tumor therapy, Int. J. Nanomedicine. 13 (2018) 7229–7249. https://doi.org/10.2147/IJN.S182197.

[4] S. Mura, J. Nicolas, P. Couvreur, Stimuli-responsive nanocarriers for drug delivery, Nat. Mater. 12 (2013) 991–1003. https://doi.org/10.1038/nmat3776.

[5] J.D. Bargh, A. Isidro-Llobet, J.S. Parker, D.R. Spring, Cleavable linkers in antibody-drug conjugates, Chem. Soc. Rev. 48 (2019) 4361–4374. https://doi.org/10.1039/c8cs00676h.

[6] L. Brülisauer, M.A. Gauthier, J.C. Leroux, Disulfide-containing parenteral delivery systems and their redox-biological fate, J. Control. Release. 195 (2014) 147–154. https://doi.org/10.1016/j.jconrel.2014.06.012.

[7] J. Li, X.L. Yang, Y.H. Liu, W.X. Wu, B.Y. Liu, N. Wang, X.Q. Yu, Chemoenzymatic synthesis of dual-responsive graft copolymers for drug delivery: Long-term stability, high loading and cell selectivity, J. Mater. Chem. B. 6 (2018) 6993–7003. https://doi.org/10.1039/c8tb01973h.

[8] Y. Zheng, Y. Shen, X. Meng, Y. Wu, Y. Zhao, C. Wu, Stabilizing p-dithiobenzyl urethane linkers without rate-limiting self-immolation for traceless drug release, ChemMedChem. 14 (2019) 1196–1203. https://doi.org/10.1002/cmdc.201900248.

[9] H. Yang, Y. Miao, L. Chen, Z. Li, R. Yang, X. Xu, Z. Liu, L.M. Zhang, X. Jiang, Redox-responsive nanoparticles from disulfide bond-linked poly-(N-ε-carbobenzyloxy-L-lysine)-grafted hyaluronan copolymers as theranostic nanoparticles for tumor-targeted MRI and chemotherapy, Int. J. Biol. Macromol. 148 (2020) 483–492. https://doi.org/10.1016/j.ijbiomac.2020.01.071.

[10] V.M. Vrudhula, J.F. MacMaster, Z. Li, D.E. Kerr, P.D. Senter, Reductively activated disulfide prodrugs of paclitaxel, Bioorganic Med. Chem. Lett. 12 (2002) 3591–3594. https://doi.org/10.1016/S0960-894X(02)00784-9.

[11] Y. Wang, X. Wang, F. Deng, N. Zheng, Y. Liang, H. Zhang, B. He, W. Dai, X. Wang, Q. Zhang, The effect of linkers on the self-assembling and anti-tumor efficacy of disulfide-linked doxorubicin drug-drug conjugate nanoparticles, J. Control. Release. 279 (2018) 136–146. https://doi.org/10.1016/j.jconrel.2018.04.019.

[12] X. Zhao, P. Liu, Reduction-responsive core-shell-corona micelles based on triblock copolymers: Novel synthetic strategy, characterization, and application as a tumor microenvironment-responsive drug delivery system, ACS Appl. Mater. Interfaces. 7 (2015) 166–174. https://doi.org/10.1021/am505531e.

[13] G. Wu, Y.-Z. Fang, S. Yang, J.R. Lupton, N.D. Turner, Glutathione metabolism and its implications for health, J. Nutr. 134 (2004) 489–492. https://doi.org/10.1093/jn/134.3.489.

[14] B. Goldenbogen, N. Brodersen, A. Gramatica, M. Loew, J. Liebscher, A. Herrmann, H. Egger, B. Budde, A. Arbuzova, Reduction-sensitive liposomes from a multifunctional lipid conjugate and natural phospholipids: reduction and release kinetics and cellular uptake, Langmuir. 27 (2011) 10820–10829. https://doi.org/10.1021/la201160y.

[15] P. Tharkar, R. Varanasi, W.S.F. Wong, C.T. Jin, W. Chrzanowski, Nano-enhanced drug delivery and therapeutic ultrasound for cancer treatment and beyond, Front. Bioeng. Biotechnol. 7 (2019) 324. https://doi.org/10.3389/FBIOE.2019.00324.

[16] V.W. Karisma, W. Wu, M. Lei, H. Liu, M.F. Nisar, M.D. Lloyd, C. Pourzand, J.L. Zhong, UVA-triggered drug release and photo-protection of skin, Front. Cell Dev. Biol. 9 (2021) 128. https://doi.org/10.3389/FCELL.2021.598717.

[17] X. Wang, Z. Xuan, X. Zhu, H. Sun, J. Li, Z. Xie, Near-infrared photoresponsive drug delivery nanosystems for cancer photo-chemotherapy, J. Nanobiotechnology. 18 (2020) 1–19. https://doi.org/10.1186/S12951-020-00668-5.

[18] Y. Liu, S. Zhu, K. Gu, Z. Guo, X. Huang, M. Wang, H.M. Amin, W. Zhu, P. Shi, GSH-activated NIR fluorescent prodrug for podophyllotoxin delivery, ACS Appl. Mater. Interfaces. 9 (2017) 29496–29504. https://doi.org/10.1021/ACSAMI.7B07091.

[19] A.G. Cheetham, R.W. Chakroun, W. Ma, H. Cui, Self-assembling prodrugs, Chem. Soc. Rev. 46 (2017) 6638–6663. https://doi.org/10.1039/c7cs00521k.

[20] C. Lin, H. He, Y. Zhang, M. Xu, F. Tian, L. Li, Y. Wang, Acetaldehyde-modified-cystine functionalized Zr-MOFs for pH/GSH dual-responsive drug delivery and selective visualization of GSH in living cells, RSC Adv. 10 (2020) 3084–3091. https://doi.org/10.1039/c9ra05741b.

[21] C. Ding, Z. Li, A review of drug release mechanisms from nanocarrier systems, Mater. Sci. Eng. C. 76 (2017) 1440–1453. https://doi.org/10.1016/j.msec.2017.03.130.

[22] J. Fang, T. Seki, H. Maeda, Therapeutic strategies by modulating oxygen stress in cancer and inflammation, Adv. Drug Deliv. Rev. 61 (2009) 290–302. https://doi.org/10.1016/j.addr.2009.02.005.

[23] N. Wu, J. Zhang, J. Zhao, K. Mu, J. Zhang, Z. Jin, J. Yu, J. Liu, Precision medicine based on

tumorigenic signaling pathways for triple-negative breast cancer, Oncol. Lett. 16 (2018) 4984–4996. https://doi.org/10.3892/ol.2018.9290.

[24] C.-H. Whang, E. Yoo, S.K. Hur, K.S. Kim, D. Kim, S. Jo, A highly GSH-sensitive SN-38 prodrug with an “OFF-to-ON” fluorescence switch as a bifunctional anticancer agent, Chem. Commun. 54 (2018) 9031–9034. https://doi.org/10.1039/C8CC05010D.

[25] L. Qiu, M. Zhu, K. Gong, J. Chen, pH-Sensitive degradable polymeric micelles for bio-triggered targeted anti-tumor drug delivery, J. Control. Release. 259 (2017) e86–e87. https://doi.org/10.1016/j.jconrel.2017.03.188.

[26] K.M. Dillon, C.R. Powell, J.B. Matson, Self-immolative prodrugs: effective tools for the controlled release of sulfur signaling species, Synlett. 30 (2019) 525–531. https://doi.org/dx.doi.org/10.13070/mm.en.2.117.

[27] C.R. Powell, K.M. Dillon, Y. Wang, R.J. Carrazzone, J.B. Matson, A persulfide donor responsive to reactive oxygen species: insights into reactivity and therapeutic potential, Angew. Chemie - Int. Ed. 57 (2018) 6324–6328. https://doi.org/10.1002/anie.201803087.

[28] M. Arslan, R. Sanyal, A. Sanyal, Thiol-reactive thiosulfonate group containing copolymers: facile entry to disulfide-mediated polymer conjugation and redox-responsive functionalizable networks, Polym. Chem. 11 (2020) 1763–1773. https://doi.org/10.1039/c9py01851d.

[29] F. Seidi, R. Jenjob, D. Crespy, Designing smart polymer conjugates for controlled release of payloads, Chem. Rev. 118 (2018) 3965–4036. https://doi.org/10.1021/acs.chemrev.8b00006.

[30] C. Shetty, A. Noronha, A. Pontarelli, C.J. Wilds, J.K. Oh, Dual-location dual-acid/glutathione-degradable cationic micelleplexes through hydrophobic modification for enhanced gene silencing, Mol. Pharm. 17 (2020) 3979–3989. https://doi.org/10.1021/acs.molpharmaceut.0c00767.

[31] A.M. Jazani, J.K. Oh, Development and disassembly of single and multiple acid-cleavable block copolymer nanoassemblies for drug delivery, Polym. Chem. 11 (2020) 2934–2954. https://doi.org/10.1039/d0py00234h.

[32] K.A. Miller, E.G. Morado, S.R. Samanta, B.A. Walker, A.Z. Nelson, S. Sen, D.T. Tran, D.J. Whitaker, R.H. Ewoldt, P. V. Braun, S.C. Zimmerman, Acid-triggered, acid-generating, and self-amplifying degradable polymers, J. Am. Chem. Soc. 141 (2019) 2838–2842. https://doi.org/10.1021/jacs.8b07705.

[33] Y. Ikuta, Y. Koseki, T. Onodera, H. Oikawa, H. Kasai, The effect of molecular structure on the anticancer drug release rate from prodrug nanoparticles, Chem. Commun. 51 (2015) 12835–12838. https://doi.org/10.1039/c5cc04164c.

[34] K. Bohn, A. Lange, J. Chmielewski, C.A. Hrycyna, Dual modulation of human P-glycoprotein and ABCG2 with prodrug dimers of the atypical antipsychotic agent paliperidone in a model of the blood-brain barrier, Mol. Pharm. 14 (2017) 1107–1119. https://doi.org/10.1021/acs.molpharmaceut.6b01044.

[35] R. Bej, P. Dey, S. Ghosh, Disulfide chemistry in responsive aggregation of amphiphilic systems, Soft Matter. 16 (2019) 11–26. https://doi.org/10.1039/c9sm01960j.

[36] F. Guo, G. Li, S. Ma, H. Zhou, X. Chen, Multi-responsive nanocarriers based on β-CD-PNIPAM star polymer coated MSN-SS-Fc composite particles, Polymers (Basel). 11 (2019) 1716. https://doi.org/10.3390/polym11101716.

[37] Y. Tian, R. Tian, L. Chen, R. Jin, Y. Feng, Y. Bai, X. Chen, Y. Tian, R. Tian, L. Chen, R. Jin, Y. Feng, Y. Bai, X. Chen, Redox-responsive nanogel with intracellular reconstruction and programmable drug release for targeted tumor therapy, Macromol. Rapid Commun. 40 (2019) 1800824. https://doi.org/10.1002/marc.201800824.

[38] T.H. Pillow, J.D. Sadowsky, D. Zhang, S.F. Yu, G. Del Rosario, K. Xu, J. He, S. Bhakta, R. Ohri, K.R. Kozak, E. Ha, J.R. Junutula, J.A. Flygare, Decoupling stability and release in disulfide bonds with antibody-small molecule conjugates, Chem. Sci. 8 (2016) 366–370. https://doi.org/10.1039/c6sc01831a.

[39] X.J. Zou, Y.C. Ma, L.E. Guo, W.X. Liu, M.J. Liu, C.G. Zou, Y. Zhou, J.F. Zhang, A lysosome-targeted fluorescent chemodosimeter for monitoring endogenous and exogenous hydrogen sulfide by in vivo imaging, 50 (2014) 13833–13836. https://doi.org/10.1039/C4CC05539J.

[40] H. Zhang, M. Li, C. Zhang, G. Zhang, J. Chao, L. Shi, Q. Yao, S. Shuang, C. Dong, The design of hydrogen sulfide fluorescence probe based on dual nucleophilic reaction and its application for bioimaging, Spectrochim. Acta - Part A Mol. Biomol. Spectrosc. 207 (2019) 150–155. https://doi.org/10.1016/j.saa.2018.09.022.

[41] H.R.M. Aitken, M.A. Brimble, D.P. Furkert, A catalytic asymmetric ene reaction for direct preparation of α-hydroxy 1,4-diketones as intermediates in natural product synthesis, Synlett. 31 (2020) 687–690. https://doi.org/10.1055/s-0037-1610748.

[42] D.J. Canney, K.D. Holland, J.A. Levine, A.C. McKeon, J.A. Ferrendelli, D.F. Covey, Synthesis and structure–activity studies of alkyl-substituted γ-butyrolactones and γ-thiobutyrolactones: ligands for the picrotoxin receptor, J. Med. Chem. 34 (1991) 1460–1467. https://doi.org/10.1021/JM00108A034.

[43] H.A. Namanja, D. Emmert, D.A. Davis, C. Campos, D.S. Miller, C.A. Hrycyna, J. Chmielewski, Toward eradicating HIV reservoirs in the brain: Inhibiting P-glycoprotein at the blood-brain barrier with prodrug abacavir dimers, J. Am. Chem. Soc. 134 (2012) 2976–2980. https://doi.org/10.1021/ja206867t.

[44] H.J. Forman, H. Zhang, A. Rinna, Glutathione: Overview of its protective roles, measurement, and biosynthesis, Mol. Aspects Med. 30 (2009) 1–12. https://doi.org/10.1016/J.MAM.2008.08.006.

[45] A. Meister, Glutathione metabolism and its selective modification, J. Biol. Chem. 263 (1988) 17205–17208. https://doi.org/10.1016/S0021-9258(19)77815-6.

[46] J.A. Burns, J.C. Butler, J. Moran, G.M. Whitesides, Selective reduction of disulfides by tris(2-carboxyethyl)phosphine, J. Org. Chem. 56 (1991) 2648–2650.

https://doi.org/10.1021/JO00008A014.

[47] O. Dmitrenko, C. Thorpe, R.D. Bach, Mechanism of SN2 disulfide bond cleavage by phosphorus nucleophiles. Implications for biochemical disulfide reducing agents, J. Org. Chem. 72 (2007) 8298–8307. https://doi.org/10.1021/JO071271W.

[48] P. Nagy, Kinetics and Mechanisms of thiol–disulfide exchange covering direct substitution and thiol oxidation-mediated pathways, Antioxid. Redox Signal. 18 (2013) 1623. https://doi.org/10.1089/ARS.2012.4973.

[49] M. Karimi, M.T. Ignasiak, B. Chan, A.K. Croft, L. Radom, C.H. Schiesser, D.I. Pattison, M.J. Davies, Reactivity of disulfide bonds is markedly affected by structure and environment: implications for protein modification and stability, Sci. Reports 2016 61. 6 (2016) 1–12. https://doi.org/10.1038/srep38572.

[50] C. Hacioglu, F. Kar, Capsaicin induces redox imbalance and ferroptosis through ACSL4/GPx4 signaling pathways in U87-MG and U251 glioblastoma cells, Metab. Brain Dis. 1 (2022) 1–16. https://doi.org/10.1007/s11011-022-00983-w.

[51] W. Zhong, T. Yan, R. Lim, L.W. Oberley, Expression of superoxide dismutases, catalase, and glutathione peroxidase in glioma cells, Free Radic. Biol. Med. 27 (1999) 1334–1345. https://doi.org/10.1016/S0891-5849(99)00181-1.

[52] Z. Zhu, S. Du, Y. Du, J. Ren, G. Ying, Z. Yan, Glutathione reductase mediates drug resistance in glioblastoma cells by regulating redox homeostasis, J. Neurochem. 144 (2018) 93–104. https://doi.org/10.1111/JNC.14250.

[53] M.D. Polewski, R.F. Reveron-Thornton, G.A. Cherryholmes, G.K. Marinov, K. Cassady, K.S. Aboody, Increased expression of system x_c^- in glioblastoma confers an altered metabolic state and temozolomide resistance, Mol. Cancer Res. 14 (2016) 1229–1242. https://doi.org/10.1158/1541-7786.MCR-16-0028.

[54] J. Wang, X. Sun, W. Mao, W. Sun, J. Tang, M. Sui, Y. Shen, Z. Gu, Tumor redox heterogeneity-responsive prodrug nanocapsules for cancer chemotherapy, Adv. Mater. 25 (2013) 3670–3676. https://doi.org/10.1002/adma.201300929.

[55] D.L. Vitale, A. Icardi, P. Rosales, F.M. Spinelli, I. Sevic, L.D. Alaniz, Targeting the tumor extracellular matrix by the natural molecule 4-methylumbelliferone: a complementary and alternative cancer therapeutic strategy, Front. Oncol. 11 (2021) 3938. https://doi.org/10.3389/fonc.2021.710061.

[56] Sigma-Aldrich, Dulbecco's Modified Eagle's Medium (DME) Formulation, Sigmaaldrich.Com [Online]. (2022). https://www.sigmaaldrich.com/CA/en/technical-documents/technical-article/cell-culture-and-cell-culture-analysis/mammalian-cell-culture/dulbecco-modified-eagle-medium-formulation.

[57] Sigma-Aldrich, RPMI-1640 Media Formulation, Sigmaaldrich.Com [Online]. (2013). https://www.sigmaaldrich.com/CA/en/technical-documents/technical-article/cell-culture-and-cell-culture-analysis/mammalian-cell-culture/media-formulations-rpmi-1640.

[58] Sigma-Aldrich, Minimum Essential Medium, Eagle, Modified Formulation, Sigmaaldrich.Com [Online]. (2022). https://www.sigmaaldrich.com/CA/en/technical-documents/technical-article/cell-culture-and-cell-culture-analysis/mammalian-cell-culture/mem-formulation.

[59] M. Johnson, Fetal bovine serum, Mater. Methods. 2 (2012). https://doi.org/10.13070/mm.en.2.117.

[60] J.I. Heger, K. Froehlich, J. Pastuschek, A. Schmidt, C. Baer, R. Mrowka, C. Backsch, E. Schleußner, U.R. Markert, A. Schmidt, Human serum alters cell culture behavior and improves spheroid formation in comparison to fetal bovine serum, Exp. Cell Res. 365 (2018) 57–65. https://doi.org/10.1016/j.yexcr.2018.02.017.

[61] G. Gstraunthaler, T. Lindl, J. Van Der Valk, A plea to reduce or replace fetal bovine serum in cell culture media, Cytotechnology. 65 (2013) 791–793. https://doi.org/10.1007/S10616-013-9633-8.

Graphical Abstract